frontiers | Frontiers in Earth Science

TYPE Original Research
PUBLISHED 28 September 2022
DOI 10.3389/feart.2022.974548

OPEN ACCESS

EDITED BY
Simona Ferrando,
University of Turin, Italy

REVIEWED BY
Andrea Maffeis,
Università di Torino—Dipartimento di Scienze della Terra, Italy
Penglei Liu,
China University of Geosciences Wuhan, China

*CORRESPONDENCE
Yi Chen,
chenyi@mail.iggcas.ac.cn

SPECIALTY SECTION
This article was submitted to Petrology, a section of the journal Frontiers in Earth Science

RECEIVED 21 June 2022
ACCEPTED 12 September 2022
PUBLISHED 28 September 2022

CITATION
Li Y-B, Chen Y, Su B, Zhang Q-H and Shi K-H (2022), Redox species and oxygen fugacity of slab-derived fluids: Implications for mantle oxidation and deep carbon-sulfur cycling.
Front. Earth Sci. 10:974548.
doi: 10.3389/feart.2022.974548

Redox species and oxygen fugacity of slab-derived fluids: Implications for mantle oxidation and deep carbon-sulfur cycling

Yi-Bing Li[1,2,3], Yi Chen[1,2,3]*, Bin Su[1,3], Qing-Hua Zhang[1,2,3] and Kai-Hui Shi[1,2,3]

[1]State Key Laboratory of Lithospheric Evolution, Institute of Geology and Geophysics, Chinese Academy of Sciences, Beijing, China, [2]University of Chinese Academy of Sciences, Beijing, China, [3]Innovation Academy for Earth Science, Chinese Academy of Sciences, Beijing, China

The generation and migration of slab-derived fluids modulate subduction zone seismicity, arc magmatism, and deep volatile cycling. However, the redox species and oxygen fugacity (fO_2) (hereafter expressed as log units relative to the fayalite–magnetite–quartz buffer, △FMQ) of slab-derived fluids are highly debated. Here we conducted phase equilibria modeling on altered oceanic crust (AOC) and serpentinites along typical subduction geotherms in the C-S-bearing system over a pressure range of 0.5–6 GPa. With the averaged compositions of AOC and serpentinite, our calculated results show that oxidized carbon-sulfur species dominate slab-derived fluids during slab subduction. As a result, slab-derived fluids are highly oxidized and at or above the typical △FMQ values of arc magmas at forearc to subarc depths. The predicted oxidized carbon and sulfur species are compatible with natural observations in fluid inclusions from many oceanic HP metamorphic rocks. More importantly, it is revealed that, the redox state of slab-derived fluids is primarily controlled by the redox budget (RB) of the slab prior to subduction. Subduction-zone thermal structure, however, only exerts a minor influence on the slab-derived fluid fO_2, which is supported by the similar fO_2 ranges in arc lavas from cold and hot subduction zones. Our models further show that, if an open system is assumed, most of carbon (>70%) and sulfur (>50%) in cold subducted AOC and serpentinite would be lost at subarc depths. Small amounts of carbon and sulfur could be transported into the deeper mantle *via* closed-system subduction and open-system cold subduction, supplying the source materials for volatile-rich intraplate magmas and superdeep diamonds.

KEYWORDS

slab-derived fluids, fluid species, oxygen fugacity, redox budget, mantle oxidation, carbon-sulfur cycle

1 Introduction

Subduction zones are a key locus of fluid generation, mass transfer, crust-mantle interaction, and arc magmatism (Manning, 2004). Slab-derived fluids transport recycling materials into the overlying mantle wedge and significantly affect the physical-chemical behaviors of the subducting slab and the fO_2 of the upper mantle and mantle-derived magmas. Slab dehydration is essential for producing intermediate-depth earthquakes and shaping plate subduction styles (Hacker et al., 2003; Chen and Ye, 2013; Zhan, 2020), and the nature and fO_2 of slab-derived fluids play crucial roles in continental crust growth, ore deposit formation, and the evolution of Earth's atmosphere (Ishihara, 2004; Jego and Pichavant, 2012; Tomkins and Evans, 2015; Duncan and Dasgupta, 2017).

Arc magmas have fO_2 of 1–4 log units higher than mid-ocean ridge basalts (Evans et al., 2012; Cottrell et al., 2021). This feature is commonly attributed to the influence of oxidized fluids released by subducting slabs. The oxidation of slab may take place during seafloor hydrothermal alteration at mid-ocean ridges or pre-trench bends before subduction (Tomkins and Evans, 2015). However, there is a continuing debate on whether the redox state of fluid speciation is oxidized or reduced. Most previous studies on fluid inclusions in high-pressure (HP) metamorphic rocks, experiments, isotope evidence, and thermodynamic calculations suggested that the slab-derived fluids are highly oxidized (Scambelluri and Philippot, 2001; Frezzotti et al., 2011; Frezzotti and Ferrando, 2015; Pons et al., 2016; Rielli et al., 2017; Gerrits et al., 2019; Walters et al., 2020a; Iacovino et al., 2020; Maurice et al., 2020; Zhang et al., 2021; Ague et al., 2022), whereas some argued for rather reduced fluids (Song et al., 2009; Frezzotti and Ferrando, 2015; Brovarone et al., 2017; Tao et al., 2018; Chen et al., 2019; Piccoli et al., 2019; Li et al., 2020). As a result, the redox state of slab-derived fluids is proposed to have a broad fO_2 range varying from △FMQ+5 to △FMQ−4 (e.g., Evans and Powell, 2015; Debret and Sverjensky, 2017; Piccoli et al., 2019; Walters et al., 2020b; Wang et al., 2020). Therefore, whether slab-derived fluids could act as an effective oxidizing agent to adjust the redox state of the mantle remain controversial.

Based on the newly developed geochemical thermodynamic model–Deep Earth Water (DEW) model (Sverjensky et al., 2014; Huang and Sverjensky, 2019), some efforts have been made to investigate the effects of thermal structure, rock lithologies, and the redox state of the pre-subduction slab on the redox state of slab-derived fluids to reconcile these two opposite views (e.g., Sverjensky et al., 2014; Walters et al., 2020a; Evans and Frost, 2021; Ague et al., 2022). For example, Sverjensky et al. (2014) found that the major carbon species in fluids equilibrated with oceanic crust are organic ($CH_3CH_2COO^-$ and $HCOO^-$) and inorganic ionic carbon species, whereas those equilibrated with peridotite generally contain CH_4 and $CO_2/HCO_3^-/CO_3^{2-}$. Walters et al. (2020a) applied a detailed thermodynamic and petrographic-based approach to sulfur-bearing eclogites and found that the aqueous S species and redox state of AOC-derived fluids are influenced by the protolith oxidation state and subduction-zone thermal structure. Both aqueous C and S species are thought to be able to sufficiently affect the oxidation state of the mantle (e.g., Evans, 2012; Sverjensky et al., 2014; Kelemen and Manning, 2015). However, the existing studies rarely treated S and C collectively and neglected the interplay between them. Therefore, further quantitative investigations in the C-S-bearing systems are needed.

Redox-sensitive elements of Fe, C, and S can contribute significantly to the redox budget (RB) of global subduction zones (Evans, 2006). In this study, we conduct thermodynamic modeling to investigate the redox-sensitive carbon and sulfur species and fO_2 in the AOC and serpentinite-derived fluids at forearc to subarc depths along cold and hot subduction geotherms. We find that slab-derived fluids are highly oxidized and mainly controlled by the source redox budget. Our new results thus provide critical information on the nature and composition of slab fluids and have implications for the C-S cycling in subduction zones.

2 Materials and methods

2.1 Thermodynamic modeling methods

We calculated pressure-temperature (P–T) pseudosections and electrolytic fluid speciation for different slab components of AOC (Staudigel et al., 1989) (in the Na_2O–CaO–K_2O–FeO–MgO–Al_2O_3–SiO_2–H_2O–CO_2–S_2–O_2 system) and serpentinite (Deschamps et al., 2013) (CaO–FeO–MgO–Al_2O_3–SiO_2–H_2O–CO_2–S_2–O_2–Cr_2O_3), using Perple_X 6.9.1 (Connolly, 2005; Galvez et al., 2015, 2016; Connolly and Galvez, 2018) and the HP62/HP622 and DEW19 thermodynamic databases (Holland and Powell, 2011; Huang and Sverjensky, 2019). The DEW model enables us to calculate equilibrium between minerals, aqueous solute, and solvent species up to 6 GPa and 1200°C (Sverjensky et al., 2014; Huang and Sverjensky, 2019), which covers our modeling P–T range (0.5–6.0 GPa and 400–1000°C). This model is not applicable to melt, although slab melting seems likely to occur in some hot subduction zones (Syracuse et al., 2010; Hernández-Uribe et al., 2020). Here we only investigated the nature of AOC- and serpentinite-derived fluids because the oceanic crust is the volumetrically largest fluid source, and the hydrated lithospheric mantle is the major source of redox budget (Evans and Tomkins, 2021). Na_2O and K_2O were neglected in the abyssal serpentinites due to their low contents (Deschamps et al., 2013). Cl is a common and important component in slab-derived fluids (e.g., Jarrard, 2003; Bekaert et al., 2021). However, recent experiments suggest that the role of Cl in enhancing the solubility and mobility of carbonates and Fe^{3+} under

subduction zone conditions is limited (Sanchez-Valle et al., 2017; Li and Wang., 2022), so we excluded Cl from the present model. The bulk compositions and solid solution models used are listed in Supplementary Table S1 and S2, respectively. The initial oxidation state of the redox-sensitive elements (Fe, C, and S) in a system is specified by the amount of excess O_2 $[0.25n(Fe^{3+})+n(C^{4+}) - 0.5n(S^{2-}) - 0.25n(S^{-}) + 1.5n(S^{6+})]$, thus requiring the oxidation state of iron, carbon, and sulfur in AOC and serpentinite (Supplementary Table S1) as prior knowledge. The lagged speciation algorithm (Connolly and Galvez, 2018), which allows the mass balance between solids and fluids, was used to derive the electrolytic fluid speciation and concentration. For conditions where all C- or S-bearing minerals are completely dissolved, we set aq_bad_results to ignore bad results in the calculation. Moreover, we resampled those results by meemum. exe and "interim_results" set to true to examine if they are equal to those calculated by werami. exe (Supplementary Figure S1). We considered the neutrally charged COHS (H_2O, CO_2, CH_4, and H_2S)-solvent model with a non-linear subdivision scheme. The equation of state (EoS) for H_2O and CO_2 is Pitzer-Sterner (PS) EoS (Pitzer and Sterner, 1995), whereas for other solvents is the Modified Redlich Kwong (MRK) (Connolly and Cesare, 1993). None of the neutral C species (e.g., $CO_{2,aq}$, $CH_{4,aq}$, $H_2CO_{3,aq}$) and S species (e.g., $H_2S_{,aq}$, $SO_{2,aq}$) were considered solutes for consistency with the use of a COHS solvent. The $MgSiC^+$ and $HFeO_2^-$ species were also excluded because of their unrealistically high concentrations at the *P–T* conditions of interest (Connolly, personal communications; Peng et al., 2020; Spranitz et al., 2022).

In this study, we calculated electrolytic fluid speciation by assuming both a closed and open system along the Honshu (cold subduction) and Cascadia (hot subduction) geotherms. Fluid fractionation in the open system follows the Rayleigh fractionation model (Connolly and Galvez, 2018; Walters et al., 2020a) at about 2°C intervals from 400°C (where major dehydration reactions get initiated) until H_2O is fully extracted from the system. The closed-system modeling does not allow fluid escape during dehydration but still provides a convenient reference for comparison (Evans and Powell, 2015; Connolly and Galvez, 2018). The two types of subduction geotherms used in this study represent a rapid convergence (8 cm/y) of ~129 Myr old crust with a slab dip of 29° and a slow convergence (3 cm/y) of ~7 Myr young crust with a slab dip of 20° (Syracuse et al., 2010), respectively. The broad *P–T* conditions considered here cover a suite of subduction zone environments.

2.2 Redox budget fluxes ($\dot{RB}$) calculation method

Although fO_2 is an important parameter that suggests whether the slab-derived fluids have the potential to oxidize the mantle or not, it is independent of the quantity of the redox-sensitive elements (e.g., Giggenbach, 1992; Evans, 2012). Therefore, slab fluid-related redox budget fluxes rather than fO_2 alone are more suitable for discussing mantle oxidation. Here, we followed the equations of Evans et al. (2012) to evaluate the oxidation capacity of the slab-derived fluids on the upper mantle.

According to the relationship between the mantle fO_2 and redox budget (Evans et al. (2012), pp. 27), we have

$$\Delta FMQ = 4.77 + 1.61 \ln \overline{RB_M} \quad (1)$$

where $\overline{RB_M}$ is the mantle redox budget in mol kg^{-1} $\overline{RB_M}$ evolves as a function of time as slab fluid-related redox budget is added to the mantle during slab subduction:

$$\overline{RB_M} = \overline{RB_{Mi}} + \frac{\dot{RB}\Delta t}{M_w} \quad (2)$$

$$\dot{RB} = \sum (S \cdot \rho \cdot h \cdot C_l) \quad (3)$$

where$\overline{RB_{Mi}}$ is the initial mantle redox budget (0.042 mol/kg, Li and Lee, 2004). $\dot{RB}$ is the slab fluid-related redox budget flux relative to the mantle reference state (Evans, 2006). Δt is time. M_W is the mass of a subduction-affected mantle wedge [5.46×10^{20} kg, Evans et al. (2012)]. S is the subducted area (km^2/year), ρ and h are the density (kg/m^3) and thickness of subducted materials, respectively. C_l is carbon and sulfur concentrations in slab-derived fluids.

3 Results

3.1 Mineral assemblage evolution

Mineral assemblages (expressed as common rock types) of AOC and serpentinite at 0.5–6 GPa and 400–1000°C are shown in Figure 1. Detailed labeled phase diagrams are provided in Supplementary Figure S2. Along the cold subduction (e.g., Honshu geotherm) (Figure 1A), lawsonite, talc, and glaucophane are the major hydrous minerals up to 670°C (2.7 GPa) in AOC. Carbon-bearing minerals include graphite and magnesite, stable at T<420°C and T<630°C, respectively. Pyrite is the only sulfur-bearing phase below 670°C. Above 670°C, the subducted AOC only contains limited H_2O contents (2–5 vol % muscovite), and all the carbon and sulfur would be incorporated into the aqueous fluid. Along the hot subducted geotherm, AOC has hydrous minerals (epidote, glaucophane, and chlorite) at temperatures lower than 780°C (2.4 GPa), with dolomite and pyrite as the only carbon- and sulfur-bearing phases below 680°C. Deep subduction of AOC along both geotherms would release ~20 vol% fluids (Supplementary Figure S3).

In the serpentinite system, mineral assemblages and proportions along different geotherms are similar (Figure 1B and Supplementary Figure S3), consistent with previous

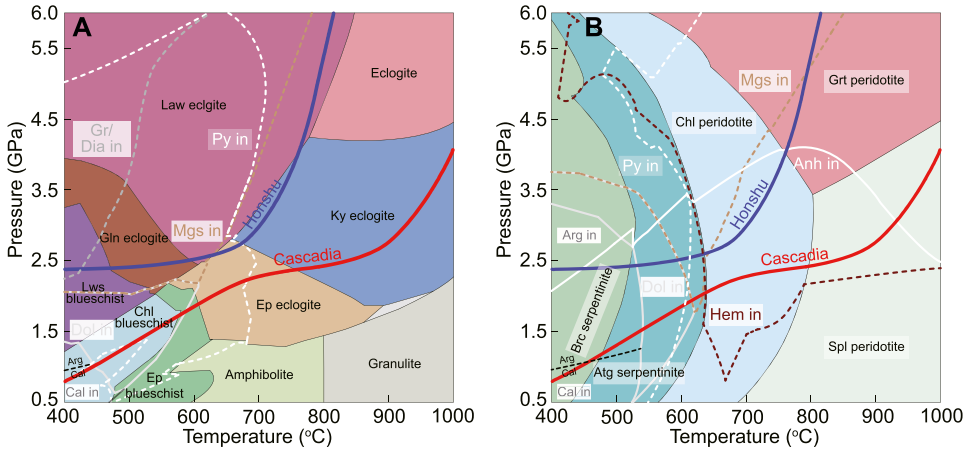

FIGURE 1
Diagrams showing the division of common rock types and the stability *P–T* fields of carboniferous and sulfurous minerals in the AOC **(A)** and serpentinite **(B)** systems, based on Supplementary Figure S2. Top-of-slab subduction geotherms for Honshu (cold) and Cascadia (hot) endmember models are after Syracuse et al. (2010). Mineral abbreviations (Whitney and Evans, 2010) used in this study can be found in Supplementary Table S2.

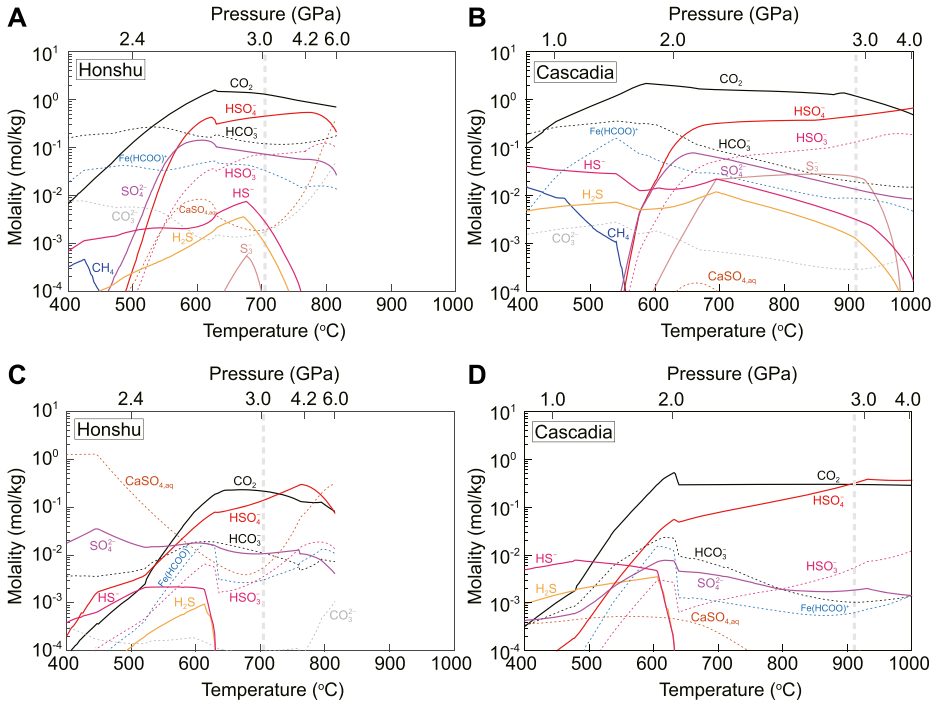

FIGURE 2
Concentrations of redox-sensitive carbon and sulfur species in the AOC **(A, B)**- and serpentinite **(C, D)**-derived fluids along the Honshu and Cascadia subduction geotherms in the closed system. These results are almost equal to those in the open system (Supplementary Figure S4). The dashed thick line marks the subarc depths, geometrically constrained by Syracuse et al. (2010).

predictions (e.g., Evans and Powell, 2015). The hydrous minerals of brucite, antigorite, and chlorite would dehydrate gradually with increasing temperature. Brucite converts to olivine at 480–520°C, where antigorite starts to dehydrate and finally transforms to olivine, orthopyroxene, and chlorite at ~630°C. Aragonite converts to dolomite between 1.5 GPa (hot

subduction) and 2.5 GPa (cold subduction) at ~530°C. Dolomite would be replaced by magnesite at ~600°C, which is close to the temperature of pyrite disappearance. All magnesite would dissolve into the aqueous fluid during antigorite breakdown, accompanied by hematite precipitation. Pyrite and anhydrite are the major sulfur-bearing phases in the serpentinite system. Pyrite is only stable at <600°C, whereas anhydrite can appear up to 750°C and 4.0 GPa in Honshu and 920°C and 3.0 GPa in Cascadia.

3.2 Electrolytic fluid speciation evolution

The composition and redox-sensitive speciation of carbon- and sulfur-bearing fluids equilibrated with subducted slab in a closed system are calculated using lagged speciation algorithm (Connolly and Galvez, 2018) (Figure 2). The open-system model (Rayleigh fractionation, Supplementary Figure S4) gives almost identical results as does the closed-system model, such similarity was also revealed by modeling for subduction zone sediment-derived fluids (Connolly and Galvez, 2018). Figure 2 only shows the redox-sensitive C- and S-bearing species in the fluid, other bulk composition-sensitive metal-complex species involving elements (Na, K, Mg, etc.) are available in Supplementary Figure S5. The major C-bearing aqueous species in the AOC-derived fluids are CO_2, HCO_3^-, $Fe(HCOO)^+$, and CO_3^{2-}, independent of subduction zone thermal structure. CH_4 only occurs at T<~450 °C (cold) or T<~550°C (hot); its concentration in the Cascadia model is 10 mmol/kg, approximately 2 orders of magnitude greater than those in the Honshu model at 450°C (Figures 2A,B). The S-bearing aqueous species are HS^--dominant at <500 °C in the Honshu model or $HS^-$and H_2S-dominant at <580°C in the Cascadia model. The concentrations of HSO_4^-, HSO_3^- and SO_4^{2-} along both geotherms drastically increase with temperature and reach a concentration level of 500–1000, 100–200, and 10–100 mmol/kg, respectively, which is 1–2 orders of magnitude greater than those of $HS^-$and H_2S. S_3^- becomes a considerable S-bearing specie only in the fluids released by hot subducted AOC; however, its concentration decreases rapidly from 30 to 0.1 mmol/kg beyond the subarc depths.

The main C-bearing species in serpentinite-derived fluids are CO_2, HCO_3^-, and $Fe(HCOO)^+$. Their concentrations in fluids increase significantly from 0.1 to 0.3 to 200–300, 0.3–4 to 1–20, and <0.1 to 10–20 mmol/kg at T<630°C, respectively. Above 630°C, these aqueous carbon species along both geotherms would not display significant concentration variations, though HCO_3^- and $Fe(HCOO)^+$ can decrease their concentrations from 10 to 1 mmol/kg and ~1 to 0.5 mmol/kg in the hot subduction model, respectively. CO_3^{2-} only occurs in the cold subduction model and has a low concentration of <0.3 mmol/kg at forearc to subarc depths (Figure 2C). The S-bearing aqueous species in serpentinite-derived fluids are complex and include $CaSO_{4,aq}$, SO_4^{2-}, HS^-, H_2S, HSO_4^-, and HSO_3^-. $HS^-$and H_2S only appear at forearc depths, whereas the HSO_4^- and HSO_3^- concentrations increase towards subarc depths. In the Honshu model, $CaSO_{4,aq}$ concentrations decrease significantly from 1000 to 7 mmol/kg in the forearc region but increase beyond subarc depths (Figure 2C). In the Cascadia model, $CaSO_{4,aq}$ concentrations are relatively low (~0.4 mmol/kg) and this specie is restricted to forearc depths (Figure 2D). SO_4^{2-} has an overall constant concentration of ~20 mmol/kg in the Honshu model but variable concentrations of 0.4–8 mmol/kg in the Cascadia model.

Although reduced species such as CH_4, HS^-, H_2S and S_3^- could reach significant concentrations of >10 mmol/kg in fluids at forearc depths, the oxidized species such as CO_2, HCO_3^-, CO_3^{2-}, HSO_4^-, HSO_3^-, and SO_4^{2-} become dominated in subarc fluids.

3.3 Oxygen fugacity of slab-derived fluids during subduction

Oxygen fugacity (fO_2), the most common variable used to quantify the redox state of slab-derived fluids, is reflected by the above-mentioned redox-sensitive species. Notably, the fO_2 values of slab-derived fluids in open and closed systems do not show significant differences (Figure 3). Overall, the AOC- and serpentinite-derived fluids along different geotherms exhibit similar fO_2 patterns from forearc to subarc depths. Compared to the fayalite–magnetite–quartz (FMQ) buffer, AOC-derived fluids have positive ~△FMQ increasing towards subarc depths (Figures 3A,B). The fO_2 values of the serpentinite-derived fluids are almost constant (~△FMQ+2) at T<~600–610°C and sharply increase by 1.5–2 log units at ~630 °C accompanied by solid C-S-bearing phase transition and hydrous mineral dehydration (Figures 3C,D).

3.4 Influence of redox budget on the fO_2 of slab-derived fluids

Redox budget (RB), a parameter featuring the initial redox state of subducted materials before subduction, refers to the total number of transferred electrons among the multivalent elements such as iron, carbon, and sulfur (Evans, 2012) relative to a reference state. It can affect fluid speciation (Evans and Powell, 2015; Walters et al., 2020a) and the fO_2 of slab-derived fluids. In this study, we used the equation of Evans (2006) RB $[n(Fe^{3+})+4n(C^{4+}) + 0n(S^{2-}) + n(S^-) + 8n(S^{6+})]$, for a reference state of Fe as Fe^{2+}, C as C^0, and S as S^{2-}) to adjust the RB values of AOC and serpentinite. To better understand the effects of bulk RB on the fO_2 of slab-derived fluids, we calculated a set of T/P-RB pseudosections (See Supplementary Figure S6 for details) along the Honshu and Cascadia subduction geotherms,

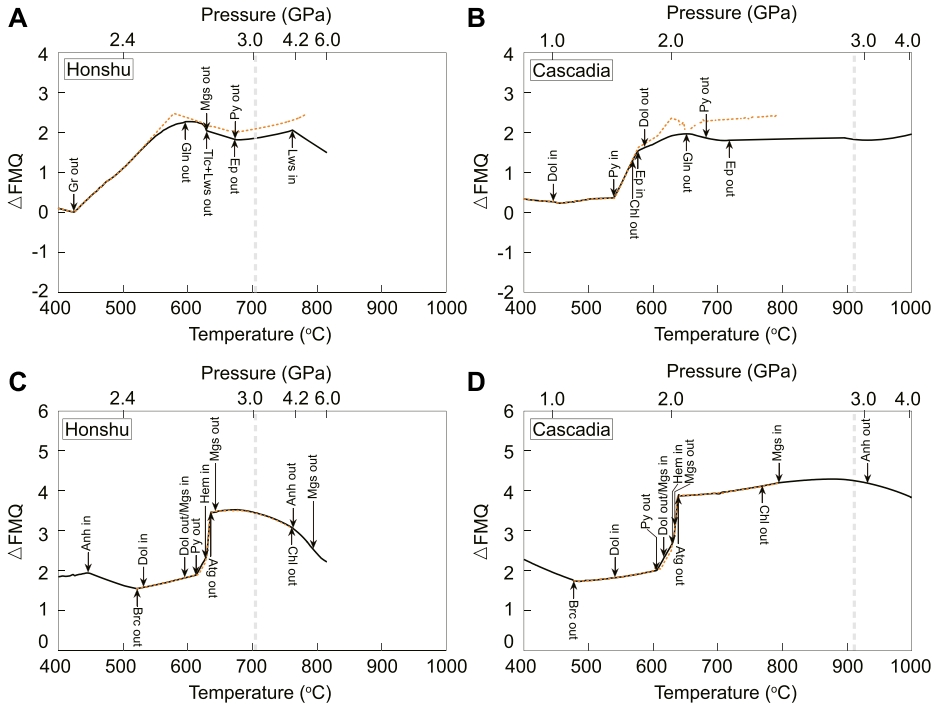

FIGURE 3
fO_2 of AOC **(A, B)**- and serpentinite **(C, D)**-derived fluids calculated along Honshu and Cascadia geotherms by assuming a closed (solid black line) and open system (dashed yellow line), respectively. △FMQ = $\log_{10}fO_2 - \log_{10}fO_{2,FMQ}$ where FMQ is the fayalite-magnetite-quartz buffer. The stability boundaries of key hydrous minerals and solid C- and S-bearing phases are shown for reference.

as well as △FMQ isopleths, in the AOC and serpentinite systems (Figure 4). Our results show that slab-derived fluids have a large fO_2 range, spanning from △FMQ+0 to △FMQ+6 in AOC and from △FMQ−6.5 to △FMQ+4.5 in serpentinite. The △FMQ isopleths exhibit vertical S-shaped patterns across the diagram, implying that the fluid fO_2 is mainly controlled by the RB of subducted reservoirs. Given a fixed RB for AOC (11.63) and MORB (9.37), the subduction of these rocks can increase the fluid fO_2 by 1.5–2 log units (Figures 4A,B). However, the fO_2 of serpentinite-derived fluid can increase significantly during subduction at low RB and temperature conditions (Figures 4C,D). The fluid fO_2 differences induced by subduction zone thermal structure are generally less than 1 log unit for the same reservoir (Figures 4A–D).

4 Discussion

4.1 Comparison with natural and experimental records for electrolytic fluid speciation

Our new models show that, with increasing PT conditions, the deep subduction-zone fluids are gradually dominated by oxidized carbon (CO_2, HCO_3^-; CO_3^{2-}) and sulfur species (HSO_4^-; HSO_3^-; SO_4^{2-}) (Figure 2), regardless of the subduction-zone thermal structure and open/closed system behavior (Figure 2, Supplementary Figures S7, S8, S4). This prediction is broadly consistent with the oxidized C-S species commonly observed in fluid inclusions from HP metamorphic rocks (Scambelluri and Philippot, 2001; Frezzotti and Ferrando, 2015). In addition, our results also suggest that $Fe(HCOO)^+$ can reach a concentration of more than 1–10 mmol/kg, which is consistent with the abiotic species observed in the solubility experiments of eclogite and peridotites (Huang and Sverjensky, 2019).

Our calculated results can also explain different fluid inclusions observed in different UHP oceanic eclogites from cold subduction zones, such as those from the western Alps and southwestern Tianshan. The former contains oxidized C and S species (HCO_3^-; CO_3^{2-}; SO_4^{2-}) (Frezzotti et al., 2011), the latter consists of reduced CH_4 and H_2 (Tao et al., 2018) or H_2S and HS^- (Li et al., 2020). The oxidized C-S species in the Alps samples could be attributed to the elevated oxidation (high RB) of subducted AOC before subduction (Supplementary Figure S7). However, abundant sulfide minerals in the Tianshan eclogites can lead to a low RB (Li et al., 2016), which would result in AOC-derived fluids dominated by reduced species of H_2S and HS^- (Supplementary Figure S7).

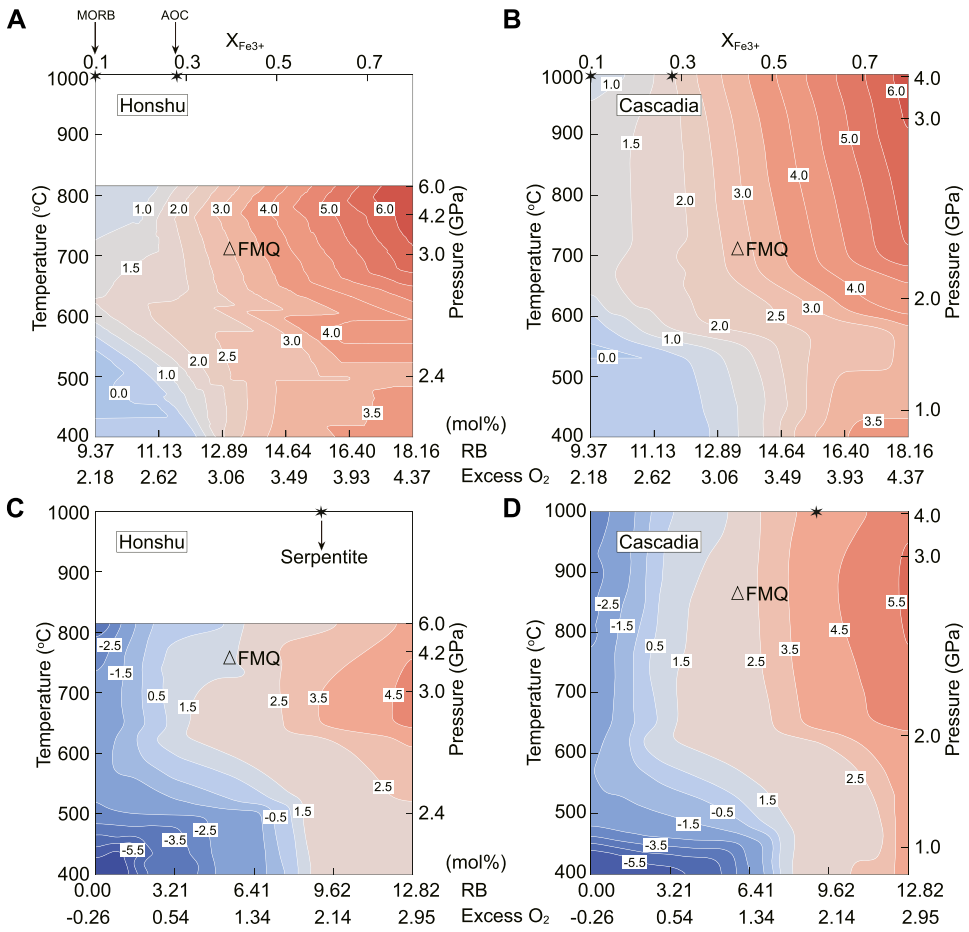

FIGURE 4
T/P-RB pseudosections showing the fO_2 variations of the AOC **(A, B)**- and serpentinite **(C, D)**-derived fluids along the Honshu and Cascadia geotherms. RB in AOC is a function of n (Fe^{3+}), mol, varying from 9.37 (X_{Fe3+}=0.1, MORB) to 18.16 (X_{Fe3+}=0.8) (Rutter, 2015) with fixed C and S contents (Staudigel et al., 1989; Evans, 2012). RB in serpentinite was adjusted by fixed contents of iron, carbon, and sulfur but with variable valence state (Evans and Powell, 2015), varying from 0.00 (assuming C is C^0, Fe is Fe^{2+} and S is S^{2-}) to 12.82 (X_{Fe3+}=1 with fixed carbon and sulfur speciation from Alt et al. (2012) and Evans (2012)). The stars represent the reference RBs of MORB (9.37) and AOC (11.63) and the averaged serpentinite (9.03).

Low-*P* experiments indicate that S_3^- is an important specie enhancing the enrichment of soft metals (Au, Cu, and Mo) in arc magmas (Pokrovski and Dubrovinsky, 2011; Pokrovski and Dubessy, 2015). However, the behavior of this species under HP conditions was not constrained in previous modeling works (Walters et al., 2020a; Evans and Frost, 2021). We predict that S_3^- in AOC-derived fluids becomes significantly abundant in hot subduction zones (Figure 2B), and can be stable under moderate fO_2 conditions (△FMQ+1 to △FMQ+2) at subarc depths (Figures 4B,Supplementary Figure S7). These predictions are consistent with the formation of large porphyry Cu-Au ore deposits commonly triggered by hot subduction processes (Cooke et al., 2005; Sun et al., 2010; Zhang et al., 2017).

Methane (CH_4) is a critical carbon specie in subduction zone fluids. CH_4-bearing fluid inclusions were discovered in oceanic eclogites and HP ophicarbonates from the southwestern Tianshan (Tao et al., 2018; Peng et al., 2020), HP-LT ophicarbonates from the western Alps (Brovarone et al., 2017, 2020) and the Alpine Corsica (Galvez et al., 2013; Brovarone et al., 2020), and metamorphosed harzburgite from the North Qilian HP-LT metamorphic belt (Song et al., 2009). All these findings indicate that abiotic CH_4 may be common in the forearc region of oceanic subduction zones. Our models show that the AOC-derived fluids would have abiotic CH_4 species at forearc depths (Figures 2A,B), and low RB values of AOC favor the CH_4 production (Supplementary Figure S7). In addition, subducted serpentinite with low RB values can also release considerable CH_4 (Supplementary Figure S8). Previous studies only considered cold subduction zones as the key reservoir of abiotic methane (e.g., Zhang et al., 2022), according to the natural HP-LT sample record in cold

oceanic subduction zones. The CH_4 production in hot subduction zones is still enigmatic due to the scarcity of exhumed HP rocks in these environments. Our models predict that, at forearc depths, hot subduction zones with low RB can produce more CH_4 than cold subduction zones (Figures 2A,B). Therefore, the forearc regions of hot subduction zones could also be a potentially key production factory of methane, which needs to be considered further during evaluating methane flux in global subduction zones.

4.2 On the fO_2 of slab-derived fluids at forearc to subarc depths

It has been long proposed that AOC-derived fluids have high fO_2 because of high Fe^{3+} content relative to sediments and serpentinites (Evans et al., 2012). However, this is challenged by the low solubility of Fe^{3+} in aqueous fluids, as revealed by several experiments (Simon et al., 2004; Sanchez-Valle et al., 2017). Our results suggest that the fO_2 of slab fluids is largely controlled by the RB values of the protoliths of subducted materials (Figure 4). Subducted MORB or sulfide-rich AOC (RB ≤9.37) could release reduced fluids (fO_2 below or near △FMQ) equilibrated with pyrite at forearc to subarc depths (Figures 4A,Supplementary Figure S7A). This prediction matches petrological records in the Tianshan pyrite-rich eclogites and HP veins (Li et al., 2016, 2020; Tao et al., 2018). With higher RB (>11.63), AOC-derived fluids are highly oxidized (△FMQ+2 to △FMQ+6), broadly consistent with the high fO_2 records in oceanic eclogites from North Qilian (△FMQ+0 to +4, Cao et al., 2011), Songduo in southern Tibet (△FMQ+2, Liu et al., 2016), and Syros in Greece (△FMQ+2 to +4, Walters et al., 2020b). Moreover, the fO_2 of AOC-derived fluids from forearc to subarc depths can increase by 2–2.5 log units during dehydration (Figures 3A,B), further implying that deep subduction AOC-derived fluids are oxidized.

The fO_2 of serpentinite-derived fluids is indicated to have a wide range of △FMQ−4 to △FMQ+5 (e.g., Peretti et al., 1992; Evans and Powell, 2015; Debret and Sverjensky, 2017), which is broadly consistent with our modeled results (Figures 4C,D). Such large variations most likely result from heterogeneous pre-subduction redox states in serpentinites (RB=2.14–12.82) (Evans and Powell, 2015). For example, at low RB (<4.81) conditions, serpentinite-derived fluids are in equilibrium with iron and pyrrhotite (Supplementary Figure S6) and have fO_2 ranging from △FMQ−6.5 to △FMQ−2.5 at <500°C, which is supported by the presence of reduced phases (awaruite, native copper, pyrrhotite, etc.) in some serpentinites (Frost, 1985; Peretti et al., 1992; Galvez et al., 2013). Our results also show that the dehydration of antigorite, accompanied with the breakdown of pyrite, would release oxidized fluids equilibrated with hematite and anhydrite with a fO_2 increase by 2 log units (from △FMQ+2 to △FMQ+4) (Figures 3C,D). This is supported by the presence of hematite in subducted serpentinites (e.g., Frost, 1985; Bach et al., 2004; Debret et al., 2015) and experimental products (Maurice et al., 2020).

Our modeling results indicate that the fO_2 of slab-derived fluids is controlled by not only Fe^{3+} but also redox-sensitive C-S species in the slab. Therefore, the RB of the subducted slab is the first-order factor affecting the oxygen fugacity of slab fluids. Subduction zone thermal structure has little influence on the fO_2 of slab-derived fluids, with variation generally below 1 log unit at fixed RB (Figure 4). This variation is much smaller than the petrological observations in oceanic eclogites and serpentinites.

4.3 Implications for mantle oxidation

To evaluate whether the oxidized fluids from dehydrating AOC and serpentinite can oxidize the subarc mantle or not, Eqs 1. and 2, and 3 were used to estimate C- and S-related oxidation fluxes released by subducted slab and timescales for mantle oxidation. We assumed a subducted area of 2.45 km^2/year (Jarrard, 2003) and densities of 3000 kg/m^3 for AOC (Bekaert et al., 2021) and 2800 kg/m^3 for serpentinite (Duan et al., 2022) with different thicknesses (Figure 5) in the calculation. Our results show that AOC- and serpentinite-related oxidation fluxes to subarc mantle are 18.6–43.3 × 10^{12} mol/year and 0.67–7.64 × 10^{12} mol/year for cold subduction and 21.3–49.8 × 10^{12} mol/year and 0.45–5.13 × 10^{12} mol/year for hot subduction. With such oxidation fluxes, the mantle fO_2 can be elevated by one to two log units on a timescale of less than 1–10 Ma. Therefore, the oxidized C-S species in the fluids are expected to oxidize Fe^{2+} in the mantle wedge (Kelley and Cottrell, 2009), which is responsible for the △FMQ to △FMQ+3 range in fO_2 reported from subarc peridotite xenoliths (Ballhaus, 1993; Parkinson and Arculus, 1999; Peslier et al., 2002; Evans et al., 2012). The occurrence of anhydrite and SO_4^{2-}-bearing inclusions in arc peridotite xenoliths (Bénard et al., 2018) also reflects the oxidized fluids penetrating the subarc mantle. Recent investigations on the Mariana arc lavas revealed that the subarc mantle gradually becomes oxidized and increases its fO_2 from typical mantle values (△FMQ−1 to 0) during subduction initiation to △FMQ≥1 after around 2–4 Ma subduction (Brounce et al., 2015). This implies that the sub-arc mantle is oxidized over the most lifetime of subduction.

Our results show that subduction zone thermal structure has limited influence on the fO_2 of slab-derived fluids. This prediction can be further tested by arc lavas from global cold and hot subduction zones (Cottrell et al., 2021), both of which show similar fO_2 average values (1.02±0.45 and 1.23±0.63) and ranges mostly spanning from △FMQ to △FMQ+3 (Supplementary Figure S9). The input of heterogeneous RB materials into subduction zones

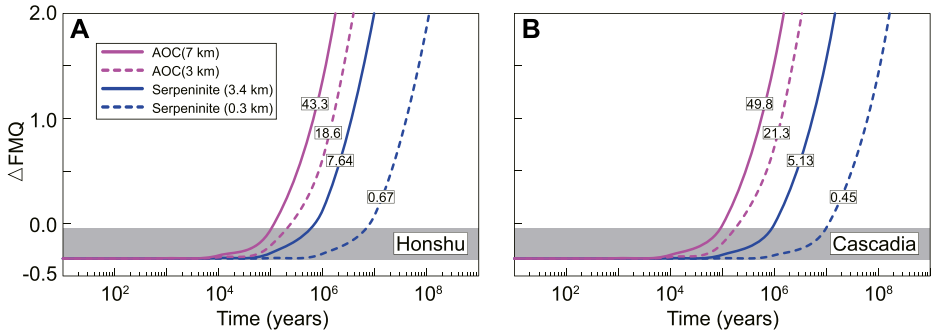

FIGURE 5
Calculated evolution of mantle logfO_2 relative to FMQ with time for the oxidation flux input from subducted AOC (**(A)**, cold) and serpentinite (**(B)**, blue) in the open system. Grey box is the initial mantle fO_2. The numbers in box represent C-and S-related oxidation fluxes (x 10^{12} mol/year) released by subducted slab. Different layer thicknesses of AOC and serpentinite are after White and Klein. (2014) and Evans (2012), respectively.

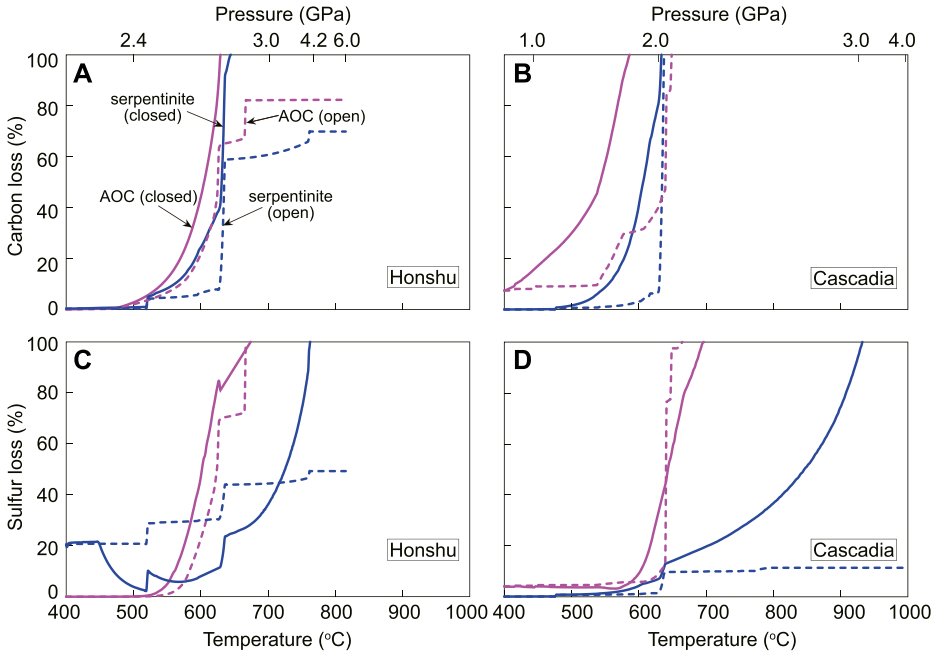

FIGURE 6
Plots of carbon and sulfur loss (carbon loss/initial carbon concentrations and sulfur loss/initial sulfur concentrations) calculated along the Honshu **(A,C)** and Cascadia geotherms **(B,D)**. The colored lines represent AOC (pink) and serpentinite (blue) systems by assuming a closed (solid line) and open (dashed line) system, respectively.

might also contribute to the large fO_2 variations (up to 3 log units) in the same arc lavas, such as Marianas and Altiplano.

For a long-term geological timescale, the atmospheric O_2 concentration was significantly increased from less than 1% to the present atmospheric level during the Ediacaran (a so-called Neoproterozoic Great Oxidation Event) (Lyons et al., 2014), which would have increased the oxidation state and redox budget of the pre-subduction slab. This is further supported by the elevated seawater sulfate during this period (Farquhar et al., 2010). After the Neoproterozoic Great Oxidation Event, the input of high RB materials into subduction zones likely induced slab fluid oxidation (Figure 4). These oxidized agents were progressively introduced into and interacted with the subarc mantle, producing high-fO_2 arc magmas and potentially generating porphyry Cu deposits (PCDs) (Richards, 2015; Sun et al., 2015). This may be one of the key mechanisms to explain why most PCDs were formed at <550 Ma (Liu et al., 2020).

4.4 Implications for deep C-S cycle in subduction zones

Based on averaged carbon and sulfur concentrations in AOC and serpentinites (Staudigel et al., 1989; Alt et al., 2012; Evans, 2012; Bekaert et al., 2021), our models can provide important constraints on the deep C-S cycle in subduction zones (Figure 6). Assuming a closed system, all carbon- and sulfur-rich phases in AOC and serpentinites would be dissolved into aqueous fluids during deep subduction beyond ~3 GPa. The closed system in subduction zones may be occasional and temporary but exists, as supported by some *in situ* HP vugs in oceanic eclogites (Angiboust and Raimondo, 2022). Subduction of the fully C-S-dissolved fluids enclosed within the slab could deliver carbon and sulfur into the deep mantle beyond subarc depths. However, for most cases, releasing fluids proceeded as an open system, which is indicated by the common occurrence of HP-veins penetrating eclogites and mantle wedge rocks (e.g., Guo et al., 2012; Plümper et al., 2017; Bloch et al., 2018). For an open system, most of carbon (>70%) and sulfur (>50%) in cold subducted AOC and serpentinites would be incorporated into aqueous fluids, which could deliver such components into the overlying mantle wedge and arc lavas (Figures 6A,C). In addition, subducted sediments may lose >40–65% of carbon and sulfur to the subarc mantle during subduction (Li et al., 2020; Stewart and Ague, 2020; Chen et al., 2021). Therefore, most subducted carbon and sulfur would complete their deep journey at subarc depths, confirming the arc system as a key region for C-S recycling (Connolly, 2005; Kelemen and Manning, 2015; Foley and Fischer, 2017; Li et al., 2020). However, the hot subducted AOC and serpentinites will lose all carbon and sulfur (except for serpentinite sulfur) at depths shallower than 70 km in the case of behaving as an open system for the fluids. (Figures 6B,D). Therefore, the closed-system subduction and open-system cold subduction can transport carbon and sulfur into the deep mantle beyond subarc depths. Besides, the heterogeneous composition (Farsang et al., 2021) and redox state (Supplementary Figures S6A, C) of carbon and sulfur in subducted slab may be also helpful for deep C-S cycling. These deep subducted carbon and sulfur would contribute to the volatile-rich mantle source of deep-seated magmas (Chalapathi Rao and Lehmann, 2011; Sakuyama et al., 2013) and the formation of superdeep diamonds with sulfide inclusions (Kaminsky, 2012; Smith et al., 2016).

5 Conclusion

Thermodynamic modeling results reveal that subducted AOC and serpentinite can produce oxidizing fluids with oxidized carbon-sulfur species and high fO_2. Moreover, the redox species and fO_2 of slab-derived fluids are mainly controlled by the redox budget of the slab before subduction but only slightly influenced by subduction-zone thermal structure. Our predictions are consistent with the petrographic and fO_2 records from exhumed high-pressure rocks, experiments, and arc lavas. Further slab fluid-related oxidation fluxes and mass balance calculations suggest that those fluids with high fO_2 can effectively oxidize the subarc mantle over geological timescales. Subducted AOC and serpentinite would lose most of carbon and sulfur to the subarc mantle, which hinders carbon-sulfur cycling in the deeper mantle.

Data availability statement

The original contributions presented in the study are included in the article/Supplementary Material, further inquiries can be directed to the corresponding author.

Author contributions

YC contributed to the conception and design of the study. Y-BL performed the modeling work. YC, Y-BL, BS, Q-HZ, and K-HS interpreted the data. Y-BL and YC wrote the manuscript.

Funding

This work was funded by the National Natural Science Foundation of China (No. 42172064, 41822202).

Acknowledgments

We thank James Connolly for the discussion on aqueous fluid modeling. Critical reviews by Andrea Maffeis and Penglei Liu and editorial handling by Simona Ferrando helped to improve the manuscript.

Conflict of interest

The authors declare that the research was conducted in the absence of any commercial or financial relationships that could be construed as a potential conflict of interest.

Publisher's note

Supplementary material

The Supplementary Material for this article can be found online at: https://www.frontiersin.org/articles/10.3389/feart.2022.974548/full#supplementary-material

References

Ague, J. J., Tassara, S., Holycross, M. E., Li, J. L., Cottrell, E., Schwarzenbach, E. M., et al. (2022). Slab-derived devolatilization fluids oxidized by subducted metasedimentary rocks. *Nat. Geosci.* 15 (4), 320–326. doi:10.1038/s41561-022-00904-7

Alt, J. C., Garrido, C. J., Shanks, W. C., III, Turchyn, A., Padrón-Navarta, J. A., Sánchez-Vizcaíno, V. L., et al. (2012). Recycling of water, carbon, and sulfur during subduction of serpentinites: A stable isotope study of cerro del almirez, Spain. *Earth Planet. Sci. Lett.* 327 (328), 50–60. doi:10.1016/j.epsl.2012.01.029

Angiboust, S., and Raimondo, T. (2022). Permeability of subducted oceanic crust revealed by eclogite-facies vugs. *Geology* 50 (8), 964–968. doi:10.1130/G50066.1

Bach, W., Garrido, C. J., Paulick, H., Harvey, J., and Rosner, M. (2004). Seawater-peridotite interactions: First insights from ODP Leg 209, MAR 15°N. *Geochem. Geophys. Geosystems* 5 (9), 744. doi:10.1029/2004GC000744

Ballhaus, C. (1993). Redox states of lithospheric and asthenospheric upper mantle. *Contributions Mineralogy Petrology* 114, 331–348. doi:10.1007/BF01046536

Bekaert, D. V., Turner, S. J., Broadley, M. W., Barnes, J. D., Halldórsson, S. A., Labidi, J., et al. (2021). Subduction-driven volatile recycling: A global mass balance. *Annu. Rev. Earth Planet. Sci.* 49, 37–70. doi:10.1146/annurev-earth-071620-055024

Bénard, A., Klimm, K., Woodland, A. B., Arculus, R. J., Wilke, M., Botcharnikov, R. E., et al. (2018). Oxidising agents in sub-arc mantle melts link slab devolatilisation and arc magmas. *Nat. Commun.* 9 (1), 1–10. doi:10.1038/s41467-018-05804-2

Bloch, W., John, T., Kummerow, J., Salazar, P., Kruger, O. S., and Shapiro, S. A. (2018). Watching dehydration: Seismic indication for transient fluid pathways in the oceanic mantle of the subducting nazca slab. *Geochem. Geophys. Geosystems* 19 (9), 3189–3207. doi:10.1029/2018gc007703

Brounce, M., Kelley, K. A., Cottrell, E., and Reagan, M. K. (2015). Temporal evolution of mantle wedge oxygen fugacity during subduction initiation. *Geology* 43 (9), 775–778. doi:10.1130/g36742.1

Brovarone, A. V., Martinez, I., Elmaleh, A., Compagnoni, R., Chaduteau, C., Ferraris, C., et al. (2017). Massive production of abiotic methane during subduction evidenced in metamorphosed ophicarbonates from the Italian Alps. *Nat. Commun.* 8, 14134. doi:10.1038/ncomms14134

Brovarone, A. V., Sverjensky, D. A., Piccoli, F., Ressico, F., Giovannelli, D., and Daniel, I. (2020). Subduction hides high-pressure sources of energy that may feed the deep subsurface biosphere. *Nat. Commun.* 11, 3880. doi:10.1038/s41467-020-17342-x

Cao, Y., Song, S. G., Niu, Y. L., Jung, H., and Jin, Z. M. (2011). Variation of mineral composition, fabric and oxygen fugacity from massive to foliated eclogites during exhumation of subducted ocean crust in the North Qilian suture zone, NW China. *J. Metamorph. Geol.* 29 (7), 699–720. doi:10.1111/j.1525-1314.2011.00937.x

Chalapathi Rao, N. V., and Lehmann, B. (2011). Kimberlites, flood basalts and mantle plumes: New insights from the deccan large igneous province. *Earth-Science Rev.* 107 (3–4), 315–324. doi:10.1016/j.earscirev.2011.04.003

Chen, C. F., Förster, M. W., Foley, S. F., and Liu, Y. S. (2021). Massive carbon storage in convergent margins initiated by subduction of limestone. *Nat. Commun.* 12 (1), 1–9. doi:10.1038/s41467-021-24750-0

Chen, Y. X., Lu, W. N., He, Y. S., Schertl, H. P., Zheng, Y. F., Xiong, J. W., et al. (2019). Tracking Fe mobility and Fe speciation in subduction zone fluids at the slab-mantle interface in a subduction channel: A tale of whiteschist from the western Alps. *Geochimica Cosmochimica Acta* 267, 1–16. doi:10.1016/j.gca.2019.09.020

Chen, Y., and Ye, K. (2013). Exhumation of subducted oceanic crust: Key issues and discussion. *Acta Petrol. Sin.* 29 (5), 1461–1478.

Connolly, J. A. D., and Cesare, B. (1993). C-O-H-S fluid composition and oxygen fugacity in graphitic metapelites. *J. Metamorph. Geol.* 11 (3), 379–388. doi:10.1111/j.1525-1314.1993.tb00155.x

Connolly, J. A. D. (2005). Computation of phase equilibria by linear programming: A tool for geodynamic modelling and its application to subduction zone decarbonation. *Earth Planet. Sci. Lett.* 236 (1–2), 524–541. doi:10.1016/j.epsl.2005.04.033

Connolly, J. A. D., and Galvez, M. E. (2018). Electrolytic fluid speciation by Gibbs energy minimization and implications for subduction zone mass transfer. *Earth Planet. Sci. Lett.* 501, 90–102. doi:10.1016/j.epsl.2018.08.024

Cooke, D. R., Hollings, P., and Walshe, J. L. (2005). Giant porphyry deposits: Characteristics, distribution, and tectonic controls. *Econ. Geol.* 100 (5), 801–818. doi:10.2113/gsecongeo.100.5.801

Cottrell, E., Birner, S. K., Brounce, M., Davis, F. A., Waters, L. E., and Kelley, K. A. (2021). "Oxygen fugacity across tectonic settings," in *Magma redox geochemistry*. Editor R. Moretti (USA: AGU Books). doi:10.1002/9781119473206.ch3

Debret, B., Bolfan-Casanova, N., Padron-Navarta, J. A., Martin-Hernandez, F., Andreani, M., Garrido, C. J., et al. (2015). Redox state of iron during high-pressure serpentinite dehydration. *Contributions Mineralogy Petrology* 169 (4), 1130. doi:10.1007/s00410-015-1130-y

Debret, B., and Sverjensky, D. A. (2017). Highly oxidising fluids generated during serpentinite breakdown in subduction zones. *Sci. Rep.* 7 (1), 1–6. doi:10.1038/s41598-017-09626-y

Deschamps, F., Godard, M., Guillot, S., and Hattori, K. (2013). Geochemistry of subduction zone serpentinites: A review. *Lithos* 178, 96–127. doi:10.1016/j.lithos.2013.05.019

Duan, W. Y., Li, X. P., Schertl, H. P., and Willner, A. P. (2022). COHS fluids released by oceanic serpentinite in subduction zones: Implications for arc-magma oxidation. *Earth Planet. Sci. Lett.* 594, 117709. doi:10.1016/j.epsl.2022.117709

Duncan, M. S., and Dasgupta, R. (2017). Rise of Earth's atmospheric oxygen controlled by efficient subduction of organic carbon. *Nat. Geosci.* 10 (5), 387–392. doi:10.1038/ngeo2939

Evans, K. A., Elburg, M. A., and Kamenetsky, V. S. (2012). Oxidation state of subarc mantle. *Geology* 40 (9), 783–786. doi:10.1130/g33037.1

Evans, K. A., and Frost, B. R. (2021). Deserpentinization in subduction zones as a source of oxidation in arcs: A reality check. *J. Petrology* 62 (3), 16. doi:10.1093/petrology/egab016

Evans, K. A., and Powell, R. (2015). The effect of subduction on the sulfur, carbon and redox budget of lithospheric mantle. *J. Metamorph. Geol.* 33 (6), 649–670. doi:10.1111/jmg.12140

Evans, K. A. (2006). Redox decoupling and redox budgets: Conceptual tools for the study of Earth systems. *Geology* 34 (6), 489–492. doi:10.1130/G22390.1

Evans, K. A. (2012). The redox budget of subduction zones. *Earth-Science Rev.* 113 (1–2), 11–32. doi:10.1016/j.earscirev.2012.03.003

Evans, K. A., and Tomkins, A. G. (2021). "Redox variables and mechanisms in subduction magmatism and volcanism," in *Magma redox geochemistry*. Editor R. Moretti (USA: AGU Books). doi:10.1002/9781119473206.ch4

Farquhar, J., Wu, N., Canfield, D. E., and Oduro, H. (2010). Connections between sulfur cycle evolution, sulfur isotopes, sediments, and base metal sulfide deposits. *Econ. Geol.* 105 (3), 509–533. doi:10.2113/gsecongeo.105.3.509

Farsang, S., Louvel, M., Zhao, C., Mezouar, M., Rosa, A. D., Widmer, R. N., et al. (2021). Deep carbon cycle constrained by carbonate solubility. *Nat. Commun.* 12 (1), 1–9. doi:10.1038/s41467-021-24533-7

Foley, S. F., and Fischer, T. P. (2017). An essential role for continental rifts and lithosphere in the deep carbon cycle. *Nat. Geosci.* 10 (12), 897–902. doi:10.1038/s41561-017-0002-7

Frezzotti, M. L., and Ferrando, S. (2015). The chemical behavior of fluids released during deep subduction based on fluid inclusions. *Am. Mineralogist* 100 (2–3), 352–377. doi:10.2138/am-2015-4933

Frezzotti, M. L., Selverstone, J., Sharp, Z. D., and Compagnoni, R. (2011). Carbonate dissolution during subduction revealed by diamond-bearing rocks from the Alps. *Nat. Geosci.* 4 (10), 703–706. doi:10.1038/ngeo1246

Frost, B. R. (1985). On the stability of sulfides, oxides, and native metals in serpentinite. *J. Petrology* 26 (1), 31–63. doi:10.1093/petrology/26.1.31

Galvez, M. E., Connolly, J. A. D., and Manning, C. E. (2016). Implications for metal and volatile cycles from the pH of subduction zone fluids. *Nature* 539, 420–424. doi:10.1038/nature20103

Galvez, M. E., Manning, C. E., Connolly, J. A. D., and Rumble, D. (2015). The solubility of rocks in metamorphic fluids: A model for rock-dominated conditions to upper mantle pressure and temperature. *Earth Planet. Sci. Lett.* 430, 486–498. doi:10.1016/j.epsl.2015.06.019

Galvez, M. E., Martinez, I., Beyssac, O., Benzerara, K., Agrinier, P., and Assayag, N. (2013). Metasomatism and graphite formation at a lithological interface in Malaspina (Alpine Corsica, France). *Contributions Mineralogy Petrology* 166 (6), 1687–1708. doi:10.1007/s00410-013-0949-3

Gerrits, A. R., Inglis, E. C., Dragovic, B., Starr, P. G., Baxter, E. F., and Burton, K. W. (2019). Release of oxidizing fluids in subduction zones recorded by iron isotope zonation in garnet. *Nat. Geosci.* 12 (12), 1029–1033. doi:10.1038/s41561-019-0471-y

Giggenbach, W. F. (1992). Magma degassing and mineral deposition in hydrothermal systems along convergent plate boundaries. *Econ. Geol.* 87, 1927–1944.

Guo, S., Ye, K., Chen, Y., Liu, J. B., Mao, Q., and Ma, Y. G. (2012). Fluid-rock interaction and element mobilization in UHP metabasalt: Constraints from an omphacite-epidote vein and host eclogites in the Dabie orogen. *Lithos* 136, 145–167. doi:10.1016/j.lithos.2011.11.008

Hacker, B. R., Peacock, S. M., Abers, G. A., and Holloway, S. D. (2003). Subduction factory 2. Are intermediate-depth earthquakes in subducting slabs linked to metamorphic dehydration reactions? *J. Geophys. Research-Solid Earth* 108 (B1), 1129. doi:10.1029/2001jb001129

Hernandez-Uribe, D., Hernandez-Montenegro, J. D., Cone, K. A., and Palin, R. M. (2020). Oceanic slab-top melting during subduction: Implications for trace-element recycling and adakite petrogenesis. *Geology* 48 (3), 216–220. doi:10.1130/g46835.1

Holland, T. J. B., and Powell, R. (2011). An improved and extended internally consistent thermodynamic dataset for phases of petrological interest, involving a new equation of state for solids. *J. Metamorph. Geol.* 29 (3), 333–383. doi:10.1111/j.1525-1314.2010.00923.x

Huang, F., and Sverjensky, D. A. (2019). Extended Deep Earth Water Model for predicting major element mantle metasomatism. *Geochimica Cosmochimica Acta* 254, 192–230. doi:10.1016/j.gca.2019.03.027

Iacovino, K., Guild, M. R., and Till, C. B. (2020). Aqueous fluids are effective oxidizing agents of the mantle in subduction zones. *Contributions Mineralogy Petrology* 175 (4), 1673. doi:10.1007/s00410-020-1673-4

Ishihara, S. (2004). "The redox state of granitoids relative to tectonic setting and earth history: the magnetite-ilmenite series 30 years later. *Earth and Environmental Science Transactions of the Royal Society of Edinburgh*95 (1–2)), 23–33. doi:10.1017/S0263593300000894

Jarrard, R. D. (2003). Subduction fluxes of water, carbon dioxide, chlorine, and potassium. *Geochem. Geophys. Geosystems* 4, 392. doi:10.1029/2002GC000392

Jego, S., and Pichavant, M. (2012). Gold solubility in arc magmas: Experimental determination of the effect of sulfur at 1000 °C and 0.4 GPa. *Geochimica Cosmochimica Acta* 84, 560–592. doi:10.1016/j.gca.2012.01.027

Kaminsky, F. (2012). Mineralogy of the lower mantle: A review of 'super-deep'mineral inclusions in diamond. *Earth-Science Rev.* 110 (1–4), 127–147. doi:10.1016/j.earscirev.2011.10.005

Kelemen, P. B., and Manning, C. E. (2015). Reevaluating carbon fluxes in subduction zones, what goes down, mostly comes up. *Proc. Natl. Acad. Sci. U. S. A.* 112 (30), E3997–E4006. doi:10.1073/pnas.1507889112

Kelley, K. A., and Cottrell, E. (2009). Water and the oxidation state of subduction zone magmas. *Science* 325 (5940), 605–607. doi:10.1126/science.11741510.1126/science.1174156

Li, J. L., Gao, J., Klemd, R., John, T., and Wang, X. S. (2016). Redox processes in subducting oceanic crust recorded by sulfide-bearing high-pressure rocks and veins (SW Tianshan, China). *Contributions Mineralogy Petrology* 171 (8–9), 1284. doi:10.1007/s00410-016-1284-2

Li, J. L., Schwarzenbach, E. M., John, T., Ague, J. J., Huang, F., Gao, J., et al. (2020). Uncovering and quantifying the subduction zone sulfur cycle from the slab perspective. *Nat. Commun.* 11 (1). doi:10.1038/s41467-019-14110-4

Li, W. C., and Wang, Q. (2022). *In situ* determination of magnesite solubility and carbon speciation in water and NaCl solutions under subduction zone conditions. *Solid Earth Sci.* 7, 200–214. doi:10.1016/j.sesci.2022.06.002

Li, Z. X. A., and Lee, C. T. A. (2004). The constancy of upper mantle fO_2 through time inferred from V/Sc ratios in basalts. *Earth Planet. Sci. Lett.* 228 (3–4), 483–493. doi:10.1016/j.epsl.2004.10.006

Liu, H., Liao, R. Q., Zhang, L. P., Li, C. Y., and Sun, W. D. (2020). Plate subduction, oxygen fugacity, and mineralization. *J. Oceanol. Limnol.* 38 (1), 64–74. doi:10.1007/s00343-019-8339-y

Liu, Y., Santosh, M., Yuan, T. Y., Li, H. Q., and Li, T. F. (2016). Reduction of buried oxidized oceanic crust during subduction. *Gondwana Res.* 32, 11–23. doi:10.1016/j.gr.2015.02.014

Lyons, T. W., Reinhard, C. T., and Planavsky, N. J. (2014). The rise of oxygen in Earth's early ocean and atmosphere. *Nature* 506 (7488), 307–315. doi:10.1038/nature13068

Manning, C. E. (2004). The chemistry of subduction-zone fluids. *Earth Planet. Sci. Lett.* 223 (1–2), 1–16. doi:10.1016/j.epsl.2004.04.030

Maurice, J., Bolfan-Casanova, N., Demouchy, S., Chauvigne, P., Schiavi, F., and Debret, B. (2020). The intrinsic nature of antigorite breakdown at 3 GPa: Experimental constraints on redox conditions of serpentinite dehydration in subduction zones. *Contributions Mineralogy Petrology* 175 (10), 1731. doi:10.1007/s00410-020-01731-y

Parkinson, I. J., and Arculus, R. J. (1999). The redox state of subduction zones: Insights from arc-peridotites. *Chem. Geol.* 160 (4), 409–423. doi:10.1016/S0009-2541(99)00110-2

Peng, W., Zhang, L., Menzel, M. D., Brovarone, A. V., Tumiati, S., Shen, T., et al. (2020). Multistage CO_2 sequestration in the subduction zone: Insights from exhumed carbonated serpentinites, SW Tianshan UHP belt, China. *Geochimica Cosmochimica Acta* 270, 218–243. doi:10.1016/j.gca.2019.11.025

Peretti, A., Dubessy, J., Mullis, J., Frost, B. R., and Trommsdorff, V. (1992). Highly reducing conditions during Alpine metamorphism of the Malenco peridotite (Sondrio, northern Italy) indicated by mineral paragenesis and H_2 in fluid inclusions. *Contributions Mineralogy Petrology* 112 (2–3), 329–340. doi:10.1007/bf00310464

Peslier, A. H., Luhr, J. F., and Post, J. (2002). Low water contents in pyroxenes from spinel-peridotites of the oxidized, sub-arc mantle wedge. *Earth Planet. Sci. Lett.* 201 (1), 69–86. doi:10.1016/S0012-821X(02)00663-5

Piccoli, F., Hermann, J., Pettke, T., Connolly, J. A. D., Kempf, E. D., and Vieira Duarte, J. F. (2019). Subducting serpentinites release reduced, not oxidized, aqueous fluids. *Sci. Rep.* 9 (1), 1–7. doi:10.1038/s41598-019-55944-8

Pitzer, K. S., and Sterner, S. M. (1995). Equations of state valid continuously from zero to extreme pressures with H_2O and CO_2 as examples. *Int. J. Thermophys.* 16 (2), 511–518. doi:10.1007/bf01441917

Plumper, O., John, T., Podladchikov, Y. Y., Vrijmoed, J. C., and Scambelluri, M. (2017). Fluid escape from subduction zones controlled by channel-forming reactive porosity. *Nat. Geosci.* 10 (2), 150–156. doi:10.1038/ngeo2865

Pokrovski, G. S., and Dubessy, J. (2015). Stability and abundance of the trisulfur radical ion in hydrothermal fluids. *Earth Planet. Sci. Lett.* 411, 298–309. doi:10.1016/j.epsl.2014.11.035

Pokrovski, G. S., and Dubrovinsky, L. S. (2011). The S3-ion is stable in geological fluids at elevated temperatures and pressures. *Science* 331 (6020), 1052–1054. doi:10.1126/science.1199911

Pons, M. L., Debret, B., Bouilhol, P., Delacour, A., and Williams, H. (2016). Zinc isotope evidence for sulfate-rich fluid transfer across subduction zones. *Nat. Commun.* 7, 13794. doi:10.1038/ncomms13794

Richards, J. P. (2015). The oxidation state, and sulfur and Cu contents of arc magmas: Implications for metallogeny. *Lithos* 233, 27–45. doi:10.1016/j.lithos.2014.12.011

Rielli, A., Tomkins, A. G., Nebel, O., Brugger, J., Etschmann, B., Zhong, R., et al. (2017). Evidence of sub-arc mantle oxidation by sulfur and carbon. *Geochem. Perspect. Lett.* 3 (2), 124–132. doi:10.7185/geochemlet.1713

Rutter, J. (2015). Characterising low temperature alteration and oxidation of the upper oceanic crust. England: University of Southampton, Ocean and Earth Science. PhD thesis.

Sakuyama, T., Tian, W., Kimura, J. I., Fukao, Y., Hirahara, Y., Takahashi, T., et al. (2013). Melting of dehydrated oceanic crust from the stagnant slab and of the hydrated mantle transition zone: Constraints from Cenozoic alkaline basalts in eastern China. *Chem. Geol.* 359, 32–48. doi:10.1016/j.chemgeo.2013.09.012

Sanchez-Valle, C., Hin, R. C., Testemale, D., Borca, C., and Grolimund, D. (2017). "Stability of oxidized iron species and the redox budget of slab-derived fluids," in *AGU Fall Meeting Abstracts*2017, V11D-01.

Scambelluri, M., and Philippot, P. (2001). Deep fluids in subduction zones. *Lithos* 55 (1–4), 213–227. doi:10.1016/s0024-4937(00)00046-3

Simon, A. C., Pettke, T., Candela, P. A., Piccoli, P. M., and Heinrich, C. A. (2004). Magnetite solubility and iron transport in magmatic-hydrothermal environments. *Geochimica Cosmochimica Acta* 68 (23), 4905–4914. doi:10.1016/j.gca.2004.05.033

Smith, E. M., Shirey, S. B., Nestola, F., Bullock, E. S., Wang, J., Richardson, S. H., et al. (2016). Large gem diamonds from metallic liquid in Earth's deep mantle. *Science* 354 (6318), 1403–1405. doi:10.1126/science.aal13010.1126/science.aal1303

Song, S. G., Su, L., Niu, Y. L., Lai, Y., and Zhang, L. F. (2009). CH_4 inclusions in orogenic harzburgite: Evidence for reduced slab fluids and implication for redox melting in mantle wedge. *Geochimica Cosmochimica Acta* 73 (6), 1737–1754. doi:10.1016/j.gca.2008.12.008

Spránitz, T., Padrón-Navarta, J. A., Szabó, C., Szabó, Á., and Berkesi, M. (2022). Abiotic passive nitrogen and methane enrichment during exhumation of subducted rocks: Primary multiphase fluid inclusions in high-pressure rocks from the cabo ortegal complex, NW Spain. *J. Metamorph. Geol.* 40, 1291–1319. doi:10.1111/jmg.12666

Staudigel, H., Hart, S. R., Schmincke, H. U., and Smith, B. M. (1989). Cretaceous ocean crust at DSDP Sites 417 and 418: Carbon uptake from weathering versus loss by magmatic outgassing. *Geochimica Cosmochimica Acta* 53 (11), 3091–3094. doi:10.1016/0016-7037(89)90189-0

Stewart, E. M., and Ague, J. J. (2020). Pervasive subduction zone devolatilization recycles CO_2 into the forearc. *Nat. Commun.* 11 (1), 1–8. doi:10.1038/s41467-020-19993-2

Sun, W. D., Huang, R. F., Li, H., Hu, Y. B., Zhang, C. C., Sun, S. J., et al. (2015). Porphyry deposits and oxidized magmas. *Ore Geol. Rev.* 65, 97–131. doi:10.1016/j.oregeorev.2014.09.004

Sun, W. D., Ling, M. X., Yang, X. Y., Fan, W. M., Ding, X., and Liang, H. Y. (2010). Ridge subduction and porphyry copper-gold mineralization: An overview. *Sci. China Earth Sci.* 53 (4), 475–484. doi:10.1007/s11430-010-0024-0

Sverjensky, D. A., Stagno, V., and Huang, F. (2014). Important role for organic carbon in subduction-zone fluids in the deep carbon cycle. *Nat. Geosci.* 7 (12), 909–913. doi:10.1038/ngeo2291

Syracuse, E. M., van Keken, P. E., and Abers, G. A. (2010). The global range of subduction zone thermal models. *Phys. Earth Planet. Interiors* 183 (1–2), 73–90. doi:10.1016/j.pepi.2010.02.004

Tao, R. B., Zhang, L. F., Tian, M., Zhu, J. J., Liu, X., Liu, J. Z., et al. (2018). Formation of abiotic hydrocarbon from reduction of carbonate in subduction zones: Constraints from petrological observation and experimental simulation. *Geochimica Cosmochimica Acta* 239, 390–408. doi:10.1016/j.gca.2018.08.008

Tomkins, A. G., and Evans, K. A. (2015). Separate zones of sulfate and sulfide release from subducted mafic oceanic crust. *Earth Planet. Sci. Lett.* 428, 73–83. doi:10.1016/j.epsl.2015.07.028

Walters, J. B., Cruz-Uribe, A. M., and Marschall, H. R. (2020a). Sulfur loss from subducted altered oceanic crust and implications for mantle oxidation. *Geochem. Perspect. Lett.* 13, 36–41. doi:10.7185/geochemlet.2011

Walters, J. B., Marschall, H., Lanari, P., and Cruz-Uribe, A. (2020b). "Oxidized slab fluids revealed in metasomatized eclogites: A case study from Syros, Greece," in *EGU general assembly conference abstracts*, 20622. doi:10.5194/egusphere-egu2020-20622

Wang, J. T., Xiong, X. L., Chen, Y. X., and Huang, F. F. (2020). Redox processes in subduction zones: Progress and prospect. *Sci. China-Earth Sci.* 63 (12), 1952–1968. doi:10.1007/s11430-019-9662-2

White, W. M., and Klein, E. M. (2014). Composition of the oceanic crust. *Treatise Geochem.* 2014, 457–496. doi:10.1016/B978-0-08-095975-7.00315-6

Whitney, D. L., and Evans, B. W. (2010). Abbreviations for names of rock-forming minerals. *Am. mineralogist* 95 (1), 185–187. doi:10.2138/am.2010.3371

Zhan, Z. W. (2020). Mechanisms and implications of deep earthquakes. *Annu. Rev. Earth Planet. Sci.* 48, 147–174. doi:10.1146/annurev-earth-053018-060314

Zhang, C. C., Sun, W. D., Wang, J. T., Zhang, L. P., Sun, S. J., and Wu, K. (2017). Oxygen fugacity and porphyry mineralization: A zircon perspective of dexing porphyry Cu deposit, China. *Geochimica Cosmochimica Acta* 206, 343–363. doi:10.1016/j.gca.2017.03.013

Zhang, L. J., Zhang, L. F., and Wang, X. (2022). Abiotic methane reserves in the Western Tianshan UHP metamorphic belt, China. *Front. Earth Sci.* 1120, 899489. doi:10.3389/feart.2022.899489

Zhang, Y. X., Gazel, E., Gaetani, G. A., and Klein, F. (2021). Serpentinite-derived slab fluids control the oxidation state of the subarc mantle. *Sci. Adv.* 7 (48), 251. doi:10.1126/sciadv.abj25110.1126/sciadv.abj2515